Contribution from the Department of Chemistry and Biochemistry, University of Notre Dame, Notre Dame, Indiana 46556, and Department of Chemistry, University of Southern California, Los Angeles, California 90089-0744

Dimerization of Metalloporphyrin π Cation Radicals. Characterization of Two Novel Dimers: $[Zn(OEP^{\bullet})(OH_2)]_2(ClO_4)_2$ and $[Ni(OEP)]_2(ClO_4)_2$

Hungsun Song,[1] Robert D. Orosz,[2] Christopher A. Reed,*[,2] and W. Robert Scheidt*[,1]

Received June 1, 1990

We report the preparation and characterization of the single-electron oxidation product of two (octaethylporphinato)metal(II) species (M = Zn, Ni). Both compounds have been crystallized and characterized by single-crystal X-ray structure determinations, IR and UV-vis spectra, and magnetic susceptibility measurements. Both species are found to form very tightly coupled dimers. The zinc complex, $[Zn(OEP^{\bullet})(OH_2)]_2(ClO_4)_2$, has two planar porphinato cores that are separated by 3.31 Å. Although the two rings are not eclipsed (the two rings are twisted 31.3° with respect to each other), the two porphinato rings do not show any lateral slipping. The porphinato core shows an unusual alternating bond distance pattern in the inner 16-membered porphyrin ring. The five-coordinate zinc ion has an axial aquo ligand. The nickel complex, $[Ni(OEP)]_2(ClO_4)_2$, contains two slightly C_{4v}-domed porphyrin rings with an average interplanar spacing of 3.19 Å. The nickel ions are displaced 0.09 Å out-of-plane (toward the dimer center) with a Ni-Ni separation of 3.01 Å. The twist angle between the two rings is 40.4°. The difference in the twist angles of the dimers leads to substantially different inter-ring contacts and probably reflects a difference in the porphinato $\pi-\pi$ interactions. The $\pi-\pi$ interactions cause strong antiferromagnetic coupling, as demonstrated by diamagnetism of the zinc dimer and probable diamagnetism of the nickel dimer. Crystal data for $[Zn(OEP^{\bullet})(OH_2)]ClO_4 \cdot C_2H_4Cl_2$: a = 29.126 (5) Å, b = 34.956 (7) Å, c = 15.670 (3) Å, orthorhombic, space group *Fddd*, V = 15,954.1 Å^3, Z = 16 (monomeric units), $ZnCl_3O_5N_4C_{38}H_{50}$, 3924 observed data, R_1 = 0.051, R_2 = 0.051, and all data at 293 K. Crystal data for $[Ni(OEP)]ClO_4 \cdot 4CH_2Cl_2$: a = 22.692 (12) Å, b = 20.978 (10) Å, c = 21.138 (4) Å, β = 115.20 (4)°, monoclinic, space group $C2/c$, V = 9104.7 ^{3}, Z = 8 (monomeric units), $NiCl_9O_4N_4C_{40}H_{52}$, 3664 observed data Å, R_1 = 0.091, R_2 = 0.115, and all data at 118 K.

In earlier work on metalloporphyrin π-cation-radical derivatives, we have investigated the nature of radical spin coupling. Examples of both intra- and intermolecular coupling have now been observed. Intramolecular coupling involves the unpaired electron of the porphyrin and a paramagnetic metal center; the nature of this coupling (antiferro- or ferromagnetic) is rationally dependent on the planarity of the porphyrin core.[3-5] Combined magnetic susceptibility measurements and X-ray structure determinations for two different crystalline forms of $[Zn(TPP^{\bullet})(OClO_3)]$[6] provided unequivocal examples of intermolecular coupling that involve only the radical spins.[7] This coupling was interpreted in terms of the well-known Bleaney-Bowers singlet-triplet coupling scheme.[8] The magnitudes of the intermolecular coupling in these two forms of $[Zn(TPP^{\bullet})(OClO_3)]$ were found to be J = −14.7 and −54.1 cm^{-1}.[7] The difference in the magnitude of the inter-ring coupling appears to be directly related to the extent of porphyrin core overlap of the dimeric π-cation-radical derivatives. The degree of interaction and overlap between the two cores is conveniently expressed in terms of the mean plane separation, the lateral shift, and the center to center distance. In $Zn(TPP^{\bullet})(OClO_3)$ dimers, the peripheral phenyl rings of one radical cation inhibit the approach of the second radical-cation complex. Hence, the TPP$^{\bullet}$ derivatives make use of an S_4 saddle-shaped ruffling of the core in order to allow the phenyl rings to be more coplanar with the porphinato ring and thus allow closer approaching rings and more strongly coupled dimers.[7] The two different crystalline forms of $[Zn(TPP^{\bullet})(OClO_3)]$ differ in the interplanar spacing and center-center distance; the derivative with the smaller spacings shows stronger coupling. In order to more completely explore the notion that the magnitude of the inter-ring coupling is proportional to the degree of overlap between two porphyrin cores, we attempted to prepare zinc π-cation derivatives with peripheral groups less sterically demanding than those of the tetraarylporphyrin series.

We have succeeded in preparing a crystalline π-cation-radical derivative of Zn(OEP). This complex forms a very strongly coupled dimer, $[Zn(OEP^{\bullet})(OH_2)]_2(ClO_4)_2$, in which the unpaired electrons on the two porphyrin rings are so strongly coupled that the dimer is diamagnetic. We have characterized this species by an X-ray structure determination and have communicated a number of unusual features found in the preliminary structure determination.[9] One of the unexpected features was the inner 16-membered ring of the porphyrin core showing localized bonding. We presumed that this unprecedented feature was a result of the very close inter-ring $\pi-\pi$ interaction. We have thus investigated other OEP$^{\bullet}$ radical systems to see whether this departure from complete delocalization in porphyrin derivatives is a general feature of tightly bonded π-cation dimers. We were successful in growing crystals of the oxidation product of Ni(OEP) but, as yet, no other OEP species capable of forming dimers. This derivative, $[Ni(OEP)]ClO_4$, also forms a dimer in the solid state. The crystal structure determination and spectroscopic characterization show that the two dimers have some significant differences. We report herein our structure determinations and other characterizations of the single-electron oxidation products of Zn(OEP) and Ni(OEP).

Experimental Section

General Information. UV-vis spectra were recorded on a Perkin-Elmer Lambda 4C spectrophotometer, and IR spectra, on a Perkin-Elmer 883 spectrometer. EPR spectra were measured on a Varian E-Line spectrometer. All solid-state samples for spectroscopy were prepared in a Vacuum Atmospheres drybox. All reactions were performed under an argon atmosphere with Schlenkware and cannula techniques. Dichloromethane and hexane were dried over CaH_2, and 1,2-dichloroethane was purified by reported procedures.[10] H_2OEP was purchased from Aldrich. In addition, a generous gift of H_2OEP was received from Prof. J. L. Sessler. Metals were inserted into the free-base H_2OEP by standard techniques.[11] Thianthrenium perchlorate was prepared by literature procedures.[12] *Caution*! These materials can detonate spontaneously and should be handled only in small quantities; other safety precautions are also warranted. We have experienced an explosion of thianthrenium perchlorate under mild heating but have had no difficulties with the porphyrin radical salts.

(1) University of Notre Dame.
(2) University of Southern California.
(3) Gans, P.; Buisson, G.; Duée, E.; Marchon, J.-C.; Erler, B. S.; Scholz, W. F.; Reed, C. A. *J. Am. Chem. Soc.* **1986**, *108*, 1223.
(4) Erler, B. S.; Scholz, W. F.; Lee, Y. J.; Scheidt, W. R.; Reed, C. A. *J. Am. Chem. Soc.* **1987**, *109*, 2644.
(5) Song, H.; Reed, C. A.; Scheidt, W. R. *J. Am. Chem. Soc.* **1989**, *111*, 6865.
(6) Abbreviations used in this paper: OEP, dianion of octaethylporphyrin; OEP$^{\bullet}$, π-cation radical of OEP; TPP, dianion of tetraphenylporphyrin; TPP$^{\bullet}$, π-cation radical of TPP; T(2,6Cl$_2$P)P, dianion of tetrakis(2,6-dichlorophenyl)porphyrin; Ct, center of the porphinato core; N_p, porphinato nitrogen.
(7) Song, H.; Rath, N. P.; Reed, C. A.; Scheidt, W. R. *Inorg. Chem.* **1989**, *28*, 1839.
(8) Bleaney, B.; Bowers, K. D. *Proc. R. Soc. London* **1952**, *A214*, 451.
(9) Song, H.; Reed, C. A.; Scheidt, W. R. *J. Am. Chem. Soc.* **1989**, *111*, 6867.
(10) Perrin, D. D.; Armarego, W. L. F.; Perrin, D. R. *Purification of Laboratory Chemicals*; Pergamon: New York, 1980.
(11) Adler, A. D.; Longo, F. R.; Kampas, F.; Kim, J. *J. Inorg. Nucl. Chem.* **1970**, *32*, 2443.
(12) Murata, Y.; Shine, H. J. *J. Org. Chem.* **1969**, *34*, 3368.

0020-1669/90/1329-4274$02.50/0

Table I. Crystal Data and Intensity Collection Parameters for $[Zn(OEP^{\bullet})(OH_2)]ClO_4 \cdot C_2H_4Cl_2$ and $[Ni(OEP)]ClO_4 \cdot 4CH_2Cl_2$

formula	$ZnCl_3O_5N_4C_{38}H_{50}$	$NiCl_9O_4N_4C_{40}H_{52}$
fw	814.58	1030.67
temp, K	293	118
space group	*Fddd*	*C2/c*
a, Å	29.126 (5)	22.692 (12)
b, Å	34.956 (7)	20.978 (10)
c, Å	15.670 (3)	21.138 (4)
β, deg		115.20 (4)
V, Å^3	15954.1	9104.7
Z	16	8
2*θ* limits, deg	3.5–54.9	4.0–53.8
radiation	Mo K*α* ($\bar{\lambda}$ = 0.71073 Å)	
background	profile analysis	
criterion for observn	$F_o > 3\sigma(F_o)$	
no. of obsd data	3924	3664
μ, mm^{-1}	0.88	1.00
R_1	0.051	0.091
R_2	0.051	0.115

Preparation of $[Zn(OEP^{\bullet})(OH_2)]ClO_4 \cdot C_2H_4Cl_2$. A 1,2-dichloroethane solution (~7 mL) of Zn(OEP) (59.6 mg, 99.7 mmol) and thianthrenium perchlorate (34.5 mg, 109.3 mmol) was stirred for 30 min in a 100-mL Schlenk flask. The solution was filtered and transferred to a 10-mL flask, which was placed in a crystallizing bottle with hexane to induce crystallization by slow vapor diffusion. After 3 or 4 days, crystals were isolated and washed with hexane (yield 78%). UV–vis (CH_2Cl_2 solution): λ_{max} 386 (Soret), 571, 637 nm. IR (KBr): ν(OEP$^{\bullet}$) 1530, 1555 cm^{-1} (weak, doublet); $\nu(ClO_4)$ 1095 (strong), 1110, 1122, 640, 630 cm^{-1}; 3450 cm^{-1} (broad peak, H_2O). When dichloromethane was used as the solvent, a different crystalline form of $[Zn(OEP^{\bullet})]^+$ was obtained.[13] IR (KBr): ν(OEP$^{\bullet}$) 1530, 1550 cm^{-1} (weak, doublet); $\nu(ClO_4)$ 1100 (broad band) with additional peaks at 1140, 640, 630 cm^{-1}.

Preparation of $[Ni(OEP)]ClO_4 \cdot 4CH_2Cl_2$. Ni(OEP) (54.8 mg, 92.9 mmol) and thianthrenium perchlorate (30 mg, 95 mmol) were placed in a 100-mL Schlenk flask. Dichloromethane (~7 mL) was added, and the solution was stirred for 1 h. The solution was filtered and transferred to a 10-mL flask, which was placed in a crystallizing bottle with hexane to induce crystallization by slow vapor diffusion. After 24 h, crystals were filtered off and washed with hexane (yield 78%). UV–vis (CH_2Cl_2 solution): λ_{max} 375 (Soret), 509, 570 nm. UV–vis (solid state): λ_{max} 371 (Soret) nm. IR (KBr): ν(OEP$^{\bullet}$) 1565 cm^{-1} (strong); $\nu(ClO_4)$ 1096 (broad), 623 (broad) cm^{-1}.

Magnetic Susceptibility Measurements. Measurements were performed on lightly compressed samples (~30 mg) in an aluminum bucket on a SHE Model 905 SQUID susceptometer at 10 kG. An apparent lattice disruption occurs when samples were ground as vigorously as is usual for magnetic susceptibility measurements. Thus, $[Zn(OEP^{\bullet})(OH_2)]ClO_4 \cdot C_2H_4Cl_2$ developed an apparent magnetic moment when the sample was vigorously ground; we interpret this as resulting from the production of magnetically isolated radicals. In order to minimize solvent loss, crystalline $[Ni(OEP)]ClO_4 \cdot 4CH_2Cl_2$ was kept in mother liquor until the sample was ready for measurement. The sample was quickly removed from the mother liquor, and the crystals were pressed into the bucket with a cylindrical rod, weighed, and within a few minutes placed in the SQUID susceptometer at low temperature. Magnetic measurements for both compounds were initiated from liquid-helium temperatures.

X-ray Diffraction Studies. $[Zn(OEP^{\bullet})(OH_2)]ClO_4 \cdot C_2H_4Cl_2$. A crystal was mounted on a glass fiber, and all X-ray examination and data collection were performed at room temperature on a Nicolet P$\bar{1}$ diffractometer. The systematic absences and Laue symmetry are only consistent with the orthorhombic space group *Fddd*. Crystal data are given in Table I; complete crystallographic details (including data collection parameters) are given in Table SI (supplementary material). Structure solution and refinement proceeded in a straightforward fashion. At convergence, the final value for the unweighted *R* was 0.051 and the weighted *R* was 0.051. Final atomic coordinates are reported in Table II; final thermal parameters and fixed hydrogen atom parameters are given in Tables SII and SIII (supplementary material).

$[Ni(OEP)]ClO_4 \cdot 4CH_2Cl_2$. A crystal was mounted on a glass fiber and placed on the diffractometer under the cold N_2 stream (−155 ± 5 °C) as soon as possible after it was taken from the mother liquor. Solvent loss and consequent crystal degradation and possible compound decomposition appeared to be a serious problem in handling $[Ni(OEP)]ClO_4 \cdot 4CH_2Cl_2$ crystals. The systematic absences and Laue symmetry are consistent with two possible space groups: *C2/c* and *Cc*. Crystal data are given in Table I; complete crystallographic details (including data collection parameters) are given in Table SI (supplementary material).

Intensity data were collected in shells of increasing 2*θ*. The 2*θ* shells contained varying numbers of reflections (typically, each shell contained 300–900 data). During the course of data collection four standard reflections were monitored after each 1 h of data collection. After about 2700 reflections had been measured a sudden decrease in the intensity of the standards was observed. After a short interval the intensity of the standard reflections again became constant but with values that were ~80% of the original intensity. All unique data to 2*θ* = 53.8° were collected. The intensity data were divided into two portions according to the intensity standards and data for each portion separately reduced by using the Blessing suite of the data reduction programs.[14] Two scale factors were assigned, one to each portion, and refined separately. A total of 3664 observed data with $F_o \geq 3.0\sigma(F_o)$, 2233 from the first segment and 1431 from the second, were used in all subsequent calculations. The centrosymmetric space group *C2/c* was initially assumed and was fully confirmed by all subsequent developments during the structure solution and refinement. The structure was solved with the direct-methods program MULTAN78;[15] most atoms of the porphinato core were found. Remaining atoms were found in subsequent difference Fourier syntheses. The structure determination showed that five separate solvent molecules, including two half-molecules, are present in an asymmetric unit. Two dichloromethane molecules were well ordered; the remainder displayed disorder of varying complexity. One disordered dichloromethane had two orientations in which one chlorine atom occupied two sites and the carbon and other chlorine atom occupied positions that were common to both sites. The second disordered dichloromethane appeared to be disordered over two different orientations as judged by Cl···Cl distances and was close to a 2-fold axis; the central carbon atom could not be located. The final dichloromethane was apparently grotesquely disordered; the several cholorine atoms of this solvent molecule were assigned occupancy factors

Table II. Fractional Coordinates for $Zn[(OEP^{\bullet})(OH_2)] \cdot C_2H_4Cl_2$[a]

atom	*x*	*y*	*z*
Zn	0.6250	0.070809 (14)	0.1250
Cl(1)	0.6250	−0.09166 (3)	0.1250
Cl(2)	0.00314 (7)	−0.08346 (6)	−0.07613 (10)
O(1)	0.61193 (10)	−0.11514 (8)	0.19509 (17)
O(2)	0.66268 (9)	−0.06811 (8)	0.14979 (20)
O(3)	0.6250	0.00956 (9)	0.1250
N(1)	0.64407 (8)	0.07803 (7)	0.25010 (14)
N(2)	0.69229 (8)	0.07798 (7)	0.09036 (15)
C(a1)	0.61494 (10)	0.07811 (8)	0.31962 (18)
C(a2)	0.68706 (10)	0.07741 (8)	0.28177 (18)
C(a3)	0.73014 (10)	0.07729 (8)	0.14411 (18)
C(a4)	0.70919 (10)	0.07866 (8)	0.01101 (19)
C(b1)	0.64170 (11)	0.07703 (8)	0.39873 (18)
C(b2)	0.68623 (10)	0.07657 (8)	0.37555 (19)
C(b3)	0.77269 (10)	0.07707 (8)	0.09392 (20)
C(b4)	0.75950 (10)	0.07829 (8)	0.01154 (19)
C(m1)	0.72750 (10)	0.07695 (9)	0.23141 (19)
C(m2)	0.68214 (10)	0.07901 (9)	−0.06402 (19)
C(11)	0.62071 (12)	0.07492 (10)	0.48666 (19)
C(12)	0.60216 (14)	0.03589 (11)	0.50997 (23)
C(21)	0.72812 (11)	0.07434 (10)	0.43197 (20)
C(22)	0.74722 (14)	0.03450 (12)	0.44210 (28)
C(31)	0.82017 (10)	0.07527 (10)	0.13063 (22)
C(32)	0.83490 (13)	0.03523 (12)	0.15540 (28)
C(41)	0.78928 (11)	0.07925 (10)	−0.06709 (21)
C(42)	0.79663 (17)	0.04126 (13)	−0.10928 (27)
C(1)	0.05093 (16)	−0.10498 (16)	−0.1239 (5)

[a] The estimated standard deviations of the least significant digits are given in parentheses.

(13) This crystalline form was not investigated in detail because of practical problems involving a too large cell. Cell constants: *a* = 23.091 Å, *b* = 37.091 Å, *c* = 39.518 Å, *β* = 91.51°, and *V* = 33833.9 Å^3.

(14) Blessing, R. H. *Crystallogr. Rev.* **1987**, *1*, 3.

(15) Programs used in this study included local modifications of Main, Hull, Lessinger, Germain, Declerq, and Woolfson's MULTAN78, Jacobson's ALLS, Zalkin's FORDAP, Busing and Levy's ORFFE and ORFLS, and Johnson's ORTEP2. Atomic form factors were from: Cromer, D. T.; Mann, J. B. *Acta Crystallogr., Sect. A.* **1968**, *A24*, 321. Real and imaginary corrections for anomalous dispersions in the form factor of the zinc, nickel, and chlorine atoms were from: Cromer, D. T.; Liberman, D. J. *J. Chem. Phys.* **1970**, *53*, 1891. Scattering factors for hydrogen were from: Stewart, R. F.; Davidson, E. R.; Simpson, W. T. *J. Chem. Phys.* **1965**, *42*, 3175. All calculations were performed on a VAX 11/730 or 3200 computer.

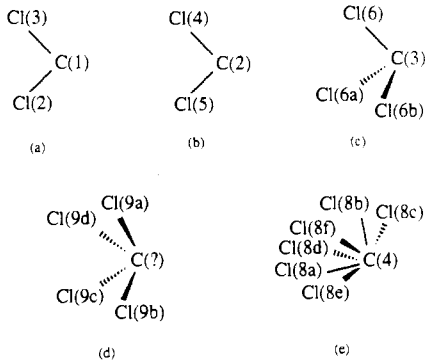

Figure 1. Stick diagrams of the dichloromethane solvate molecules in $[Ni(OEP)]ClO_4$, showing the atomic labels assigned as well as schematically depicting the nature of the disorder in (c)–(e). The molecules labeled b and d are half-occupancy molecules and are close to the boundary between two asymmetric units of structure; the symmetry operators are an inversion center and a 2-fold axis, respectively.

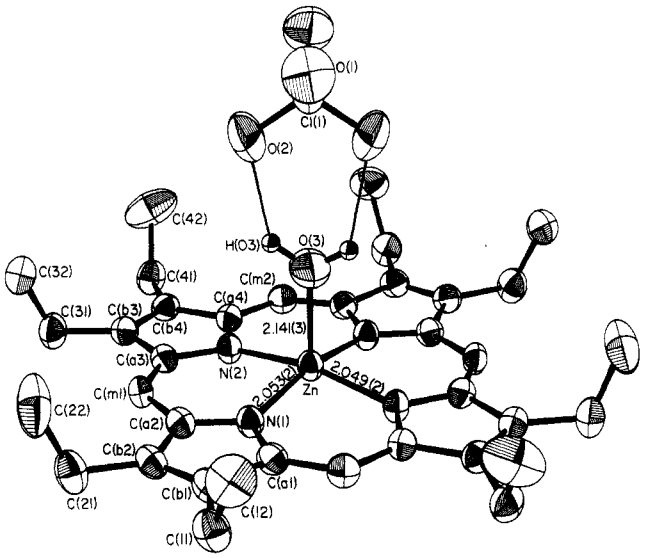

Figure 2. ORTEP diagram of $[Zn(OEP^{\bullet})(OH_2)]ClO_4$, displaying the atom-labeling scheme used throughout the paper. Bond distances in the coordination group are also shown. Ellipsoids are contoured at the 50% probability level in this and all subsequent ORTEP drawings.

from the difference Fourier peak heights and then adjusted so that the combined occupancy factors/thermal parameters had reasonable values. The five solvent molecules are schematically depicted in Figure 1, which shows atom labels as well as the disorder model employed for three of the solvent molecules.

The structure was refined to convergence with anisotropic temperature factors for all nonhydrogen atoms except the C_a's and C_b's of the porphyrin core and atoms of the disordered solvent molecules that were not well separated from each other. The hydrogen atoms were idealized as fixed contributors (C–H = 0.95 Å; $B(H) = 1.2B(C)$). The final model included 485 variables, and there were 7.6 data per variable. At convergence, the final value for the unweighted R was 0.091 and the weighted R was 0.115. A final difference Fourier synthesis was judged free of significant features with the largest peak having a height of 0.54 e/Å^3. Final atomic coordinates are given in Table III, and final tables of anisotropic thermal parameters and fixed hydrogen atom coordinates are given in Tables SIV and SV of the supplementary material.

Results

Structure of $[Zn(OEP^{\bullet})(OH_2)]ClO_4$. The molecular structure of $[Zn(OEP^{\bullet})(OH_2)]ClO_4$ is shown in Figure 2. The molecule has a crystallographically imposed 2-fold axis along the Zn–OH_2 axis. Although the imposed symmetry of the molecule does not lead to any conditions on the planarity of the porphinato core, the porphyrin ring is essentially planar with the largest deviation of any atom from the mean plane of the 24-atom core equal to 0.05 Å. The displacement of the zinc(II) atom from the mean plane of the porphinato core is 0.24 Å, a value smaller than that typically observed in five-coordinate zinc porphyrinates. Figure 3a is a formal diagram of the porphinato core showing the displacements of each atom from the mean plane of the porphinato core. On the left-hand side of this figure, the information for $[Zn(OEP^{\bullet})(OH_2)]ClO_4$ is given, while the same or similar information is given for $[Ni(OEP)]ClO_4$ on the right-hand side of the diagram. The side-by-side illustration given here (and sub-

Table III. Fractional Coordinates for $[Ni(OEP)]ClO_4 \cdot 4CH_2Cl_2$[a]

atom	x	y	z
Ni	0.45332 (7)	0.43241 (6)	0.67371 (7)
Cl(1)	0.16485 (17)	0.43740 (15)	0.28445 (19)
O(1)	0.1540 (10)	0.3855 (7)	0.3190 (12)
O(2)	0.1520 (9)	0.4945 (6)	0.3097 (10)
O(3)	0.1240 (8)	0.4311 (8)	0.2164 (9)
O(4)	0.2280 (7)	0.4391 (7)	0.2902 (9)
N(1)	0.3850 (4)	0.3937 (4)	0.6934 (4)
N(2)	0.4216 (4)	0.5174 (4)	0.6819 (4)
N(3)	0.5186 (4)	0.4721 (4)	0.6498 (4)
N(4)	0.4838 (4)	0.3481 (4)	0.6626 (4)
C(a1)	0.3712 (5)	0.3296 (5)	0.6918 (5)
C(a2)	0.3378 (5)	0.4225 (5)	0.7064 (5)
C(a3)	0.3693 (5)	0.5314 (5)	0.6973 (6)
C(a4)	0.4432 (5)	0.5761 (5)	0.6719 (6)
C(a5)	0.5290 (5)	0.5373 (5)	0.6440 (5)
C(a6)	0.5652 (5)	0.4424 (5)	0.6345 (5)
C(a7)	0.5358 (5)	0.3341 (5)	0.6479 (5)
C(a8)	0.4575 (5)	0.2907 (5)	0.6667 (5)
C(b1)	0.3122 (5)	0.3198 (5)	0.7034 (5)
C(b2)	0.2928 (5)	0.3779 (5)	0.7125 (6)
C(b3)	0.3592 (6)	0.6019 (6)	0.6959 (6)
C(b4)	0.4043 (6)	0.6275 (6)	0.6786 (6)
C(b5)	0.5817 (5)	0.5458 (5)	0.6233 (6)
C(b6)	0.6019 (5)	0.4878 (5)	0.6165 (6)
C(b7)	0.5426 (5)	0.2649 (5)	0.6442 (6)
C(b8)	0.4946 (5)	0.2387 (5)	0.6545 (6)
C(m1)	0.3314 (5)	0.4882 (5)	0.7112 (6)
C(m2)	0.4947 (5)	0.5848 (5)	0.6548 (5)
C(m3)	0.5738 (5)	0.3774 (5)	0.6356 (5)
C(m4)	0.4046 (5)	0.2819 (5)	0.6798 (6)
C(11)	0.2811 (6)	0.2565 (6)	0.7004 (7)
C(12)	0.2332 (7)	0.2392 (7)	0.6230 (8)
C(21)	0.2340 (6)	0.3961 (7)	0.7221 (7)
C(22)	0.1788 (7)	0.4199 (8)	0.6553 (8)
C(31)	0.3047 (7)	0.6318 (6)	0.7039 (7)
C(32)	0.2401 (7)	0.6298 (7)	0.6399 (7)
C(41)	0.4129 (8)	0.6953 (6)	0.6660 (8)
C(42)	0.3798 (11)	0.7087 (6)	0.5857 (9)
C(51)	0.6022 (6)	0.6100 (5)	0.6075 (6)
C(52)	0.5563 (6)	0.6350 (6)	0.5354 (6)
C(61)	0.6541 (6)	0.4694 (6)	0.5916 (6)
C(62)	0.6227 (6)	0.4517 (6)	0.5129 (6)
C(71)	0.5938 (6)	0.2320 (5)	0.6267 (6)
C(72)	0.5749 (6)	0.2280 (7)	0.5494 (6)
C(81)	0.4741 (8)	0.1688 (6)	0.6481 (10)
C(82)	0.4194 (11)	0.1540 (11)	0.5732 (15)
C(1)	0.2535 (9)	0.1047 (11)	0.4988 (12)
C(2)	0.498 (3)	0.0356 (26)	0.4814 (26)
C(3)	0.3028 (9)	0.1352 (12)	0.1215 (12)
C(4)	0.4568 (12)	0.1674 (9)	0.2909 (10)
Cl(2)	0.2635 (3)	0.02324 (26)	0.48356 (28)
Cl(3)	0.17677 (23)	0.12291 (25)	0.48348 (22)
Cl(4)	0.4453 (12)	−0.0316 (10)	0.4767 (7)
Cl(5)	0.5553 (6)	0.0406 (6)	0.5670 (10)
Cl(6)	0.25000 (28)	0.18934 (25)	0.11318 (26)
Cl(7a)	0.3125 (4)	0.1242 (4)	0.0493 (4)
Cl(7b)	0.3776 (6)	0.1202 (6)	0.1075 (9)
Cl(8a)	0.4135 (7)	0.2355 (5)	0.3257 (7)
Cl(8b)	0.4530 (17)	0.1500 (16)	0.3883 (11)
Cl(8c)	0.5012 (8)	0.1326 (7)	0.3801 (12)
Cl(8d)	0.4727 (10)	0.2529 (9)	0.3607 (11)
Cl(8e)	0.3790 (16)	0.2134 (14)	0.2995 (17)
Cl(8f)	0.4411 (4)	0.1967 (4)	0.3349 (4)
Cl(9a)	0.0229 (12)	0.5249 (12)	0.1728 (13)
Cl(9b)	0.0731 (13)	0.4901 (13)	0.3796 (13)
Cl(9c)	−0.0247 (17)	0.5301 (19)	0.2571 (21)
Cl(9d)	−0.0050 (24)	0.4755 (25)	0.2760 (23)

[a] The estimated standard deviations of the least significant digits are given in parentheses.

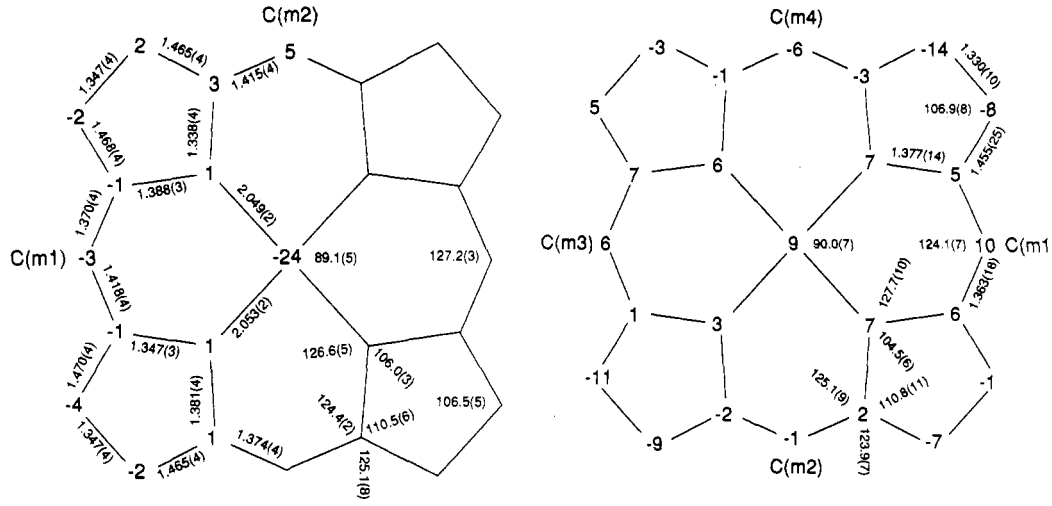

Figure 3. (a) Left: Formal diagram of the porphinato core in the $[Zn(OEP^{\bullet})(OH_2)]ClO_4$ molecule, displaying the displacement, in units of 0.01 Å, of each atom from the mean plane of the porphinato core. The displacements of the 2-fold-related atoms have the same magnitude and sign. Values of the crystallographically unique individual bond distances in the core are displayed. (b) Right: Formal diagram of the porphinato core in the $[Ni(OEP)]ClO_4$ molecule, displaying the displacement, in units of 0.01 Å, of each atom from the mean plane of the porphinato core. Also displayed in (b) are the averaged values of the bond distances and angles for the chemically unique parameters of the core. The numbers in parentheses in both diagrams are the estimated standard deviations of the particular values. Positive values of displacement are toward the center of the two rings.

sequently) is intended to allow for direct comparisons of the strucural aspects for the zinc and nickel complexes. Figure 3a shows the displacements of the crystallographically unique atoms of the core; the 2-fold-related atoms of the other half of the core have displacements of identical magnitude and sign.

In the solid state $[Zn(OEP^{\bullet})(OH_2)]ClO_4$ forms a tight cofacial π–π dimer, as displayed in Figure 4a. The interplanar separation between the mean plane of the two porphyrin cores is 3.31 Å. All peripheral ethyl groups point outward from the region between the two porphyrin rings. The view given in Figure 5a shows the complete absence of any lateral shift between the two cofacial porphyrin rings in this dimer. Figure 5a also displays a view down one of the crystallographically required 2-fold axis of the dimeric unit. The dimer has an overall required symmetry of D_2-222. The other two required 2-fold axes of the dimer are mutually perpendicular and are parallel and between the two porphyrin planes of Figure 4a. The symmetry requirements demand that the two porphinato rings are exactly parallel.

The average Zn–N_p distance is 2.051 (3) Å; the Zn–$O(OH_2)$ distance is 2.141 (3) Å. Figure 3a also shows the crystallographically unique bond distances in the porphinato core. Complete listings of bond distances and bond angles for $[Zn(OEP^{\bullet})(OH_2)]ClO_4$ are available in Table IV.

Structure of $[Ni(OEP)]ClO_4$. The molecular structure of the $[Ni(OEP)]^+$ cation is displayed in Figure 6. The cation has a modestly "C_{4v}-domed" porphinato core, which appears to be the result of a dimeric interaction in the solid state. The edge-on view of Figure 4b shows some aspects of the domed core conformation and, in addition, shows some other features of the dimer conformation in the solid state. The two porphyrin cores are clearly seen to saucer away from each other but with the two nickel atoms moving toward each other in the dimer. The Ni···Ni distance is 3.011 (4) Å, while the average separation of the two 24-atom planes is only 3.19 Å. Quantitative aspects of the domed core conformation are seen in the formal diagram (Figure 3b), which shows the displacement of each atom from the mean plane of the 24-atom core. Positive values of displacement are toward the center of the pair of rings, and thus, the nickel and porphinato nitrogen atoms are slightly above the mean plane, while C_b atoms are saucered away below the mean plane. Alternatively, the core doming can be described by noting the average displacements of various groups of atoms from the mean plane of the four nitrogen atoms: Ni, 0.04 Å; eight C_a's, −0.04 Å; four C_m's −0.03 Å; eight C_b's, −0.11 Å.

$[Ni(OEP)]ClO_4$ also forms a tight dimer with no lateral shift in the solid state, as shown in Figure 5. The average Ni–N_p bond length is 1.949 (6) Å, which is slightly shorter than those of planar

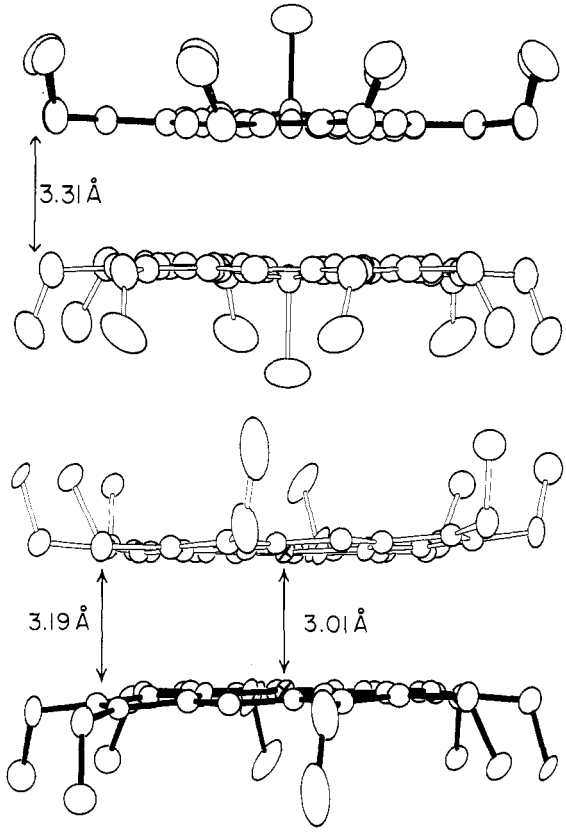

Figure 4. (a) Top: Edge-on view of the cofacial $[Zn(OEP^{\bullet})(OH_2)]_2(ClO_4)_2$ dimer, showing the essential planarity of the dimer. The interplanar separation is given. (b) Bottom: Edge-on view of the dimer of $[Ni(OEP)]_2(ClO_4)_2$, showing the saucering of the halves of the dimer toward each other. The average interplanar spacing and the Ni···Ni separation are shown.

nickel porphyrin complexes. Complete tabulations of bond distances and angles are given in Table V.

Magnetic Measurements. Temperature-dependent magnetic susceptibility measurements down to 6 K showed that $[Zn(OEP^{\bullet})(OH_2)]_2(ClO_4)_2$ is strictly diamagnetic. A temperature-independent magnetic moment of 0.30 ± 0.02 μ_B per dimer was ascribed to an ~0.83% paramagnetic impurity. Room-temperature diamagnetism sets a lower limit of −1000 cm^{-1} for the value of $2J$, the singlet–triplet energy gap. Similar measurements for

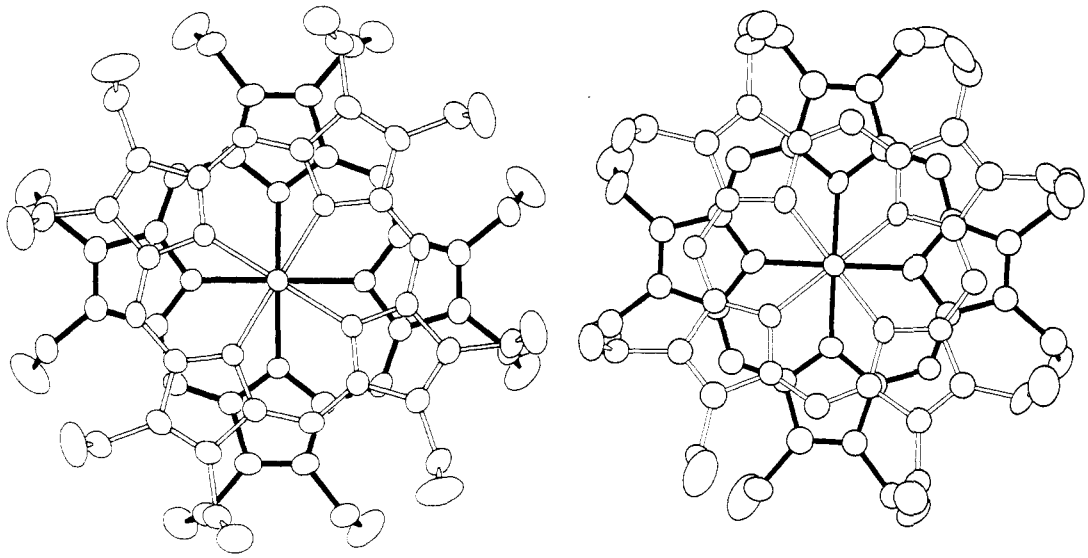

Figure 5. (a) Left: View down the 2-fold axis of the $[Zn(OEP^{\bullet})(OH_2)]_2(ClO_4)_2$ dimer, showing the orientation of the two rings with respect to each other. (b) Right: Same view for the $[Ni(OEP)]_2(ClO_4)_2$ dimer.

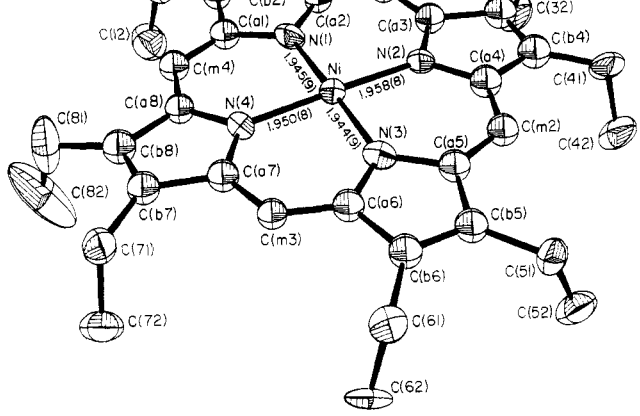

Figure 6. ORTEP diagram of the $[Ni(OEP)]ClO_4$ cation, displaying the atom-labeling scheme used throughout the paper. Bond distances in the coordination group are also shown.

$[Ni(OEP)]_2(ClO_4)_2$ showed that the compound has apparent residual paramagnetism that decreases with decreasing temperature. For various samples, the room-temperature moment was $\sim 2.0 \pm 0.2\ \mu_B$ per *dimeric* unit decreasing to $\sim 0.7\ \mu_B$ at 6 K. The compound also exhibits an EPR signal with $g = 2.002$; the intensity of the signal decreased with decreasing temperature. Listings of typical experimental susceptibility data are given as Tables SVI and SVII of the supplementary material.

Discussion

$[Zn(OEP^{\bullet})(OH_2)]ClO_4$. We first consider the coordination group geometry and synthesis of $[Zn(OEP^{\bullet})(OH_2)]ClO_4$. The complex has a five-coordinate zinc ion in which the five donors are the four porphinato nitrogen atoms and an axial aquo ligand. The molecule has a crystallographically required 2-fold symmetry along the axial Zn–O bond. The aquo ligand is apparently derived from residual water in the 1,2-dichloroethane solvent. Despite the likely variability of water content of the solvent, the crystalline preparation from dichloroethane has been found to be reproducible. Preparation from dichloromethane solution perhaps yields the anhydrous complex (with a coordinated perchlorate ion), as judged from the IR spectrum. As noted earlier, this crystalline form was not examined because of the large size of the unit cell.

The average $Zn-N_p$ distance is 2.051 (3) Å, and the metal atom displacement is 0.24 Å; both values are significantly smaller than those found for the five-coordinate imidazole and pyridine adducts of neutral zinc(II) octaethylporphyrin, where $Zn-N_p = 2.067$ Å and metal atom displacement = 0.42 Å.[16,17] These coordination group parameters are also smaller than those found for several tetraarylporphyrin species.[18] Indeed, the $Zn-N_p$ distances are

Table IV. Bond Distances and Angles in $[Zn(OEP^{\bullet})(OH_2)]ClO_4 \cdot C_2H_4Cl_2$[a]

A. Bond Lengths (Å)

Zn–N(1)	2.0530 (23)	C(a2)–C(b2)	1.470 (4)
Zn–N(2)	2.0491 (23)	C(a3)–C(m1)	1.370 (4)
Zn–O(3)	2.141 (3)	C(a3)–C(b3)	1.468 (4)
Cl(1)–O(1)	1.4231 (25)	C(a4)–C(m2)	1.415 (4)
Cl(1)–O(2)	1.4258 (25)	C(a4)–C(b4)	1.465 (4)
N(1)–C(a1)	1.381 (4)	C(b1)–C(b2)	1.347 (4)
N(1)–C(a2)	1.347 (3)	C(b3)–C(b4)	1.347 (4)
N(2)–C(a3)	1.388 (3)	C(11)–C(b1)	1.509 (4)
N(2)–C(a4)	1.338 (4)	C(11)–C(12)	1.512 (5)
C(a1)–C(m2)′	1.374 (4)	C(21)–C(22)	1.508 (5)
C(a1)–C(b1)	1.465 (4)	C(31)–C(32)	1.515 (5)
C(a2)–C(m1)	1.418 (4)	C(41)–C(42)	1.499 (5)
Zn···Zn	3.7886 (12)		

B. Bond Angles (deg)

N(2)ZnN(2)	165.94 (13)	N(2)C(a3)C(b3)	110.21 (24)
N(2)ZnN(1)	88.80 (9)	N(2)C(a4)C(m2)	124.59 (27)
N(2)ZnN(1)	89.47 (9)	N(2)C(a4)C(b4)	111.25 (25)
N(2)ZnO(3)	97.03 (7)	C(m2)C(a4)C(b4)	124.15 (27)
N(1)ZnO(3)	97.06 (7)	C(b2)C(b1)C(a1)	106.53 (26)
O(1)Cl(1)O(1)′	109.55 (25)	C(b1)C(b2)C(a2)	106.57 (26)
O(1)Cl(1)O(2)	109.19 (17)	C(b4)C(b3)C(a3)	105.82 (25)
O(1)′Cl(1)O(2)	109.72 (17)	C(b3)C(b4)C(a4)	106.90 (26)
O(2)Cl(1)O(2)′	109.47 (25)	C(a3)C(m1)C(a2)	127.03 (27)
C(a2)N(1)C(a1)	106.29 (23)	C(a1)′C(m2)C(a4)	127.45 (27)
C(a2)N(1)Zn	126.96 (19)	C(b2)C(b1)C(11)	129.47 (28)
C(a1)N(1)Zn	125.97 (19)	C(a1)C(b1)C(11)	123.94 (27)
C(a4)N(2)C(a3)	105.80 (23)	C(b1)C(b2)C(21)	128.41 (29)
C(a4)N(2)Zn	126.90 (19)	C(a2)C(b2)C(21)	124.99 (27)
C(a3)N(2)Zn	126.65 (19)	C(b4)C(b3)C(31)	129.19 (28)
C(m2)′C(a1)N(1)	124.25 (26)	C(a3)C(b3)C(31)	124.99 (27)
C(m2)′C(a1)C(b1)	125.83 (27)	C(b3)C(b4)C(41)	128.31 (28)
N(1)C(a1)C(b1)	109.92 (24)	C(a4)C(b4)C(41)	124.79 (27)
N(1)C(a2)C(m1)	124.56 (26)	C(b1)C(11)C(12)	114.16 (28)
N(1)C(a2)C(b2)	110.69 (26)	C(b2)C(21)C(22)	114.06 (29)
C(m1)C(a2)C(b2)	124.75 (26)	C(b3)C(31)C(32)	113.48 (28)
C(m1)C(a3)N(2)	124.17 (26)	C(b4)C(41)C(42)	115.03 (29)
C(m1)C(a3)C(b3)	125.62 (27)		

[a] The numbers in parentheses are the estimated standard deviations. Primed and unprimed symbols denote a pair of atoms related by the 2-fold axis.

(16) Brennan, T. D.; Scheidt, W. R. *Acta Crystallogr., Sect. C* **1988**, *C44*, 478.
(17) Cullen, D. L.; Meyer, E. F., Jr. *Acta Crystallogr., Sect. B* **1976**, *B32*, 2259.

Table V. Bond Lengths and Angles in $[Ni(OEP)]ClO_4 \cdot 4CH_2Cl_2$[a]

A. Bond Lengths (Å)

Ni-N(1)	1.945 (9)	Ni-N(2)	1.958 (8)	C(b5)-C(b6)	1.329 (14)	C(b7)-C(b8)	1.316 (15)
Ni-N(3)	1.944 (9)	Ni-N(4)	1.950 (8)	C(b1)-C(11)	1.492 (15)	C(b2)-C(21)	1.483 (15)
Cl(1)-O(1)	1.391 (14)	Cl(1)-O(2)	1.391 (11)	C(b3)-C(31)	1.457 (16)	C(b4)-C(41)	1.473 (16)
Cl(1)-O(3)	1.345 (14)	Cl(1)-O(4)	1.386 (12)	C(b5)-C(51)	1.509 (14)	C(b6)-C(61)	1.534 (15)
N(1)-C(a1)	1.376 (13)	N(1)-C(a2)	1.358 (12)	C(b7)-C(71)	1.526 (15)	C(b8)-C(81)	1.528 (17)
N(2)-C(a3)	1.389 (13)	N(2)-C(a4)	1.375 (13)	C(11)-C(12)	1.573 (19)	C(21)-C(22)	1.518 (20)
N(3)-C(a5)	1.403 (13)	N(3)-C(a6)	1.379 (12)	C(31)-C(32)	1.514 (19)	C(41)-C(42)	1.562 (22)
N(4)-C(a7)	1.374 (12)	N(4)-C(a8)	1.361 (12)	C(51)-C(52)	1.526 (16)	C(61)-C(62)	1.551 (16)
C(a1)-C(b1)	1.474 (15)	C(a1)-C(m4)	1.343 (14)	C(71)-C(72)	1.506 (16)	C(81)-C(82)	1.571 (30)
C(a2)-C(b2)	1.430 (14)	C(a2)-C(m1)	1.394 (14)	C(1)-Cl(2)	1.770 (21)	C(1)-Cl(3)	1.674 (20)
C(a3)-C(b3)	1.495 (15)	C(a3)-C(m1)	1.365 (15)	C(2)-Cl(4)	1.82 (6)	C(2)-Cl(5)	1.73 (5)
C(a4)-C(b4)	1.438 (15)	C(a4)-C(m2)	1.375 (14)	C(3)-Cl(6)	1.605 (25)	C(3)-Cl(7a)	1.650 (24)
C(a5)-C(b5)	1.449 (14)	C(a5)-C(m2)	1.342 (14)	C(3)-Cl(7b)	1.870 (25)	C(4)-Cl(8a)	2.04 (2)
C(a6)-C(b6)	1.421 (14)	C(a6)-C(m3)	1.376 (13)	C(4)-Cl(8b)	2.13 (3)	C(4)-Cl(8c)	1.87 (3)
C(a7)-C(b7)	1.465 (14)	C(a7)-C(m3)	1.353 (14)	C(4)-Cl(8d)	2.25 (3)	C(4)-Cl(8e)	2.09 (3)
C(a8)-C(b8)	1.466 (14)	C(a8)-C(m4)	1.355 (14)	C(4)-Cl(8f)	1.28 (2)	Cl(9a)-Cl(9c)	2.45 (5)
C(b1)-C(b2)	1.336 (14)	C(b3)-C(b4)	1.338 (16)	Cl(9b)-Cl(9d)	2.17 (5)		

B. Bond Angles (deg)

N(1)NiN(2)	90.3 (3)	N(1)NiN(3)	177.4 (4)	N(4)C(a7)C(m3)	125.4 (9)	N(4)C(a8)C(b8)	110.3 (9)
N(1)NiN(4)	90.1 (3)	N(2)NiN(3)	89.0 (3)	C(b8)C(a8)C(m4)	124.1 (10)	N(4)C(a8)C(m4)	125.6 (9)
N(2)NiN(4)	178.3 (4)	N(3)NiN(4)	90.5 (3)	C(a1)C(b1)C(b2)	105.9 (9)	C(b2)C(b1)C(11)	129.7 (10)
O(1)Cl(1)O(2)	111.1 (10)	O(1)Cl(1)O(3)	106.8 (13)	C(a1)C(b1)C(11)	124.3 (9)	C(a2)C(b2)C(b1)	107.0 (10)
O(1)Cl(1)O(4)	112.5 (11)	O(2)Cl(1)O(3)	109.4 (11)	C(b1)C(b2)C(21)	128.8 (11)	C(a2)C(b2)C(21)	124.1 (10)
O(2)Cl(1)O(4)	108.8 (10)	O(3)Cl(1)O(4)	108.2 (11)	C(a3)C(b3)C(b4)	105.9 (10)	C(b4)C(b3)C(31)	130.1 (11)
NiN(1)C(a1)	126.6 (7)	NiN(1)C(a2)	128.9 (8)	C(a3)C(b3)C(31)	123.6 (10)	C(a4)C(b4)C(b3)	107.4 (11)
C(a1)N(1)C(a2)	104.4 (8)	NiN(2)C(a3)	126.7 (7)	C(b3)C(b4)C(41)	127.7 (11)	C(a4)C(b4)C(41)	124.9 (11)
NiN(2)C(a4)	129.3 (7)	C(a3)N(2)C(a4)	104.0 (8)	C(a5)C(b5)C(b6)	106.7 (9)	C(b6)C(b5)C(51)	129.8 (10)
NiN(3)C(a5)	128.0 (7)	NiN(3)C(a6)	127.8 (7)	C(a5)C(b5)C(51)	123.3 (9)	C(a6)C(b6)C(b5)	108.3 (10)
C(a5)N(3)C(a6)	104.2 (8)	NiN(4)C(a7)	127.1 (7)	C(b5)C(b6)C(61)	128.3 (10)	C(a6)C(b6)C(61)	123.3 (9)
NiN(4)C(a8)	127.4 (7)	C(a7)N(4)C(a8)	105.4 (8)	C(a7)C(b7)C(b8)	106.9 (9)	C(b8)C(b7)C(71)	128.3 (10)
N(1)C(a1)C(b1)	110.2 (9)	C(b1)C(a1)C(m4)	123.6 (10)	C(a7)C(b7)C(71)	124.6 (9)	C(a8)C(b8)C(b7)	107.2 (10)
N(1)C(a1)C(m4)	126.2 (10)	N(1)C(a2)C(b2)	112.5 (9)	C(b7)C(b8)C(81)	128.9 (11)	C(a8)C(b8)C(81)	123.6 (10)
C(b2)C(a2)C(m1)	122.8 (9)	N(1)C(a2)C(m1)	124.8 (9)	C(a2)C(m1)C(a3)	123.2 (10)	C(a4)C(m2)C(a5)	124.4 (10)
N(2)C(a3)C(b3)	110.2 (9)	C(b3)C(a3)C(m1)	123.8 (10)	C(a6)C(m3)C(a7)	124.9 (9)	C(a8)C(m4)C(a1)	123.9 (10)
N(2)C(a3)C(m1)	126.1 (10)	N(2)C(a4)C(b4)	112.5 (9)	C(b1)C(11)C(12)	110.8 (10)	C(b2)C(21)C(22)	113.1 (10)
C(b4)C(a4)C(m2)	123.5 (10)	N(2)C(a4)C(m2)	123.9 (10)	C(b3)C(31)C(32)	115.6 (11)	C(b4)C(41)C(42)	109.3 (12)
N(3)C(a5)C(b5)	109.7 (9)	C(b5)C(a5)C(m2)	125.0 (10)	C(b5)C(51)C(52)	112.6 (9)	C(b6)C(61)C(62)	111.1 (10)
N(3)C(a5)C(m2)	125.3 (10)	N(3)C(a6)C(b6)	110.9 (9)	C(b7)C(71)C(72)	113.2 (10)	C(b8)C(81)C(82)	111.1 (15)
C(b6)C(a6)C(m3)	125.0 (9)	N(3)C(a6)C(m3)	124.1 (9)	Cl(2)C(1)Cl(3)	112.9 (11)	Cl(4)C(2)Cl(5)	106.8 (29)
N(4)C(a7)C(b7)	110.1 (9)	C(b7)C(a7)C(m3)	124.5 (10)	Cl(6)C(3)Cl(7a)	112.6 (12)	Cl(6)C(3)Cl(7b)	141.9 (12)

[a] The estimated standard deviations of the least significant digits are given in parentheses.

between those of four-coordinate zinc complexes (average 2.036 Å)[19] and six-coordinate derivatives (average 2.055 Å).[20,21] Both of these classes have the zinc atom centered in the porphyrin plane. These parameters, especially the decreased metal atom displacement, are consistent with the π–π interaction acting as the equivalent of a weak sixth ligand. Such effects have been previously noted for the $[Zn(TPP^{\bullet})(OClO_3)]$ π–π dimers[7] and for π-arene complexation.[22]

The axial Zn–O distance of 2.141 (3) Å is a bit longer than the value of 2.089 (5) Å observed for the Z–O(*N*-methylpyrrolidone) distance[18d] in five-coordinate $Zn(T(2,6Cl_2P)P)L$. It is comparable to the 2.13–2.14-Å Zn–O($OClO_3$) distances observed in two of the three $[Zn(TPP^{\bullet})(OClO_3)]$ complexes[7] and longer than the third (2.079 Å).[28] The axial water ligand in $[Zn(OEP^{\bullet})(OH_2)]_2(ClO_4)_2$ appears to be hydrogen bonded to the perchlorate counterion with an O···O distance of 2.954 Å (see Figure 2).

Although OEP π cation radicals have been known for some time,[23] the crystal structure of $[Zn(OEP^{\bullet})(OH_2)]ClO_4$ shows that it forms a cofacial π–π dimer with several significant and novel features. First, the two porphyrin rings in the dimer interact in an exceptionally strong manner with an interplanar separation between the two planar porphyrin rings of 3.31 Å. The interaction between the rings is unsupported by any obvious bond. Second, the absence of any lateral shift between the cofacial porphyrin rings is unprecedented. Third, despite the strong interaction between the two rings, the cores are essentially planar, as seen in Figures 3a and 4a. Fourth, the bond distances in the inner 16-membered ring of the porphyrin cores show a pattern more typical of an alternant hydrocarbon rather than a completely delocalized system. Finally, the crystalline material is diamagnetic.

The interplanar spacing of 3.31 Å is slightly smaller than the 3.35-Å value of graphite,[24] but graphite has much larger C···C separations between sheets (3.62 Å) compared to ~3.3 Å for several inter-ring interactions in $[Zn(OEP^{\bullet})(OH_2)]_2(ClO_4)_2$. The absence of any lateral shift is unprecedented, as all previously characterized, tight π–π interacting porphyrins (interplanar separations of ~3.3 Å) exhibit lateral shifts of 1.5 Å or more.[25,26]

(18) (a) Collins, D. M.; Hoard, J. L. *J. Am. Chem. Soc.* **1970**, *92*, 3761. (b) Bobrik, M. A.; Walker, F. A. *Inorg. Chem.* **1980**, *19*, 3383. (c) Hatano, K.; Kawasaki, K.; Munakata, S.; Iitaka, Y. *Bull. Chem. Soc. Jpn.* **1987**, *60*, 1985. (d) Williamson, M. M.; Prosser-McCartha, C. M.; Mukundan, S., Jr.; Hill, C. L. *Inorg. Chem.* **1988**, *27*, 1061.
(19) (a) Simonis, U.; Walker, F. A.; Lee, P. L.; Hanquet, B. J.; Meyerhoff, D. J.; Scheidt, W. R. *J. Am. Chem. Soc.* **1987**, *109*, 2659. (b) Scheidt, W. R.: Mondal, J. U.; Eigenbrot, C. W.; Adler, A.; Radonovich, L. J.; Hoard, J. L. *Inorg. Chem.* **1986**, *25*, 795. (c) Scheidt, W. R.; Kastner, M. E.; Hatano, K. *Inorg. Chem.* **1978**, *17*, 706.
(20) Scheidt, W. R.; Eigenbrot, C. W.; Ogiso, M.; Hatano, K. *Bull. Chem. Soc. Jpn.* **1987**, *60*, 3529.
(21) Schauer, C. K.; Anderson, O. P.; Eaton, S. S.; Eaton, G. R. *Inorg. Chem.* **1985**, *24*, 4082.
(22) Williamson, M. M.; Hill, C. L. *Inorg. Chem.* **1987**, *26*, 4155.
(23) (a) Fuhrhop, J.-H.; Mauzerall, D. *J. Am. Chem. Soc.* **1969**, *91*, 4174. (b) Fajer, J.; Borg, D. C.; Forman, A.; Dolphin, D.; Felton, R. H. *J. Am. Chem. Soc.* **1970**, *92*, 3451. (c) Fuhrhop, J.-H.; Wasser, P.; Riesner, D.; Mauzerall, D. *J. Am. Chem. Soc.* **1972**, *94*, 7996.
(24) Cotton, F. A.; Wilkinson, G. *Advanced Inorganic Chemistry*; 5th ed.; John Wiley: New York, 1988; pp 236–237.
(25) Scheidt, W. R.; Lee, Y. J. *Struct. Bonding (Berlin)* **1987**, *64*, 1.
(26) However, an eclipsed cofacial structure was one of two different possibilities suggested by Fuhrhop et al.[23c] for the structure of the Zn(OEP) radical.

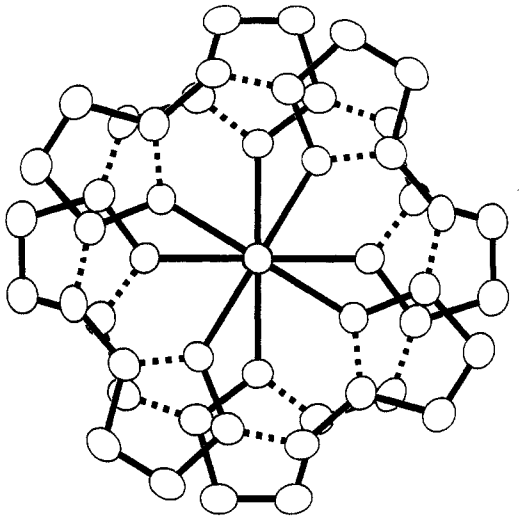

Figure 7. Diagram illustrating the relative positions of the long (full) and short (broken) bonds in the inner 16-membered ring of the porphinato cores of $[Zn(OEP^{\bullet})(OH_2)]_2(ClO_4)_2$.

Only species with metal–metal bonds (vide infra) have closely spaced porphyrin rings with no lateral shift. The porphyrin core is almost planar (Figure 3a); the largest deviation of any atom from the mean plane of the 24-atom core has the value 0.05 Å. A careful examination of the displacements of the C_a and C_m atoms with respect to their closest contact with atoms of the opposite ring reveals an unexpected result. Only *one* of the six such closest unique contacts is larger than it would be with a completely planar core. In other words, the core deformations bring inter-ring atoms *closer* together. Although the perpendicular decreases are small (0.02–0.04 Å), they are completely unexpected.

The interaction between the two porphyrin rings is much more intimate than any found for analogous TPP dimers. Indeed, such TPP dimers have been termed "incipient" dimers.[28] For the three $Zn(TPP^{\bullet})(OClO_3)$ dimers of known structure,[7,28] the interplanar separations ranged from 3.57 to 3.70 Å and the Ct···Ct distances ranged from 4.82 to 6.54 Å, substantially larger than the 3.31-Å value for $[Zn(OEP^{\bullet})(OH_2)]_2(ClO_4)_2$. The out-of-plane displacement of the Zn atom in $[Zn(OEP^{\bullet})(OH_2)]_2(ClO_4)_2$ is comparable to that in the more tightly interacting $Zn(TPP^{\bullet})(OClO_3)$ dimers and gives evidence that the second porphyrin ring acts as a weak (sixth) axial ligand as noted earlier.

The bond distance pattern of the inner 16-membered ring of the porphyrin cores of the dimer is quite unusual. There are two quite distinct sets of C_a–N and C_a–C_m bond distances. The average C_a–N distances of the two classes are 1.343 (6) and 1.385 (5) Å, while the C_a–C_m distances are 1.372 (3) and 1.417 (2) Å. The two types of bonds alternate around the ring, as shown in Figure 7, where the short lengths are depicted by the broken bonds. Such bond length variation has not been previously observed in porphyrin complexes.[29] In typical porphyrin structures, these bonds are equivalent, and thus, the observed pattern is inconsistent with the usual completely delocalized system. Figure 7 clearly shows that the short bonds in the porphyrin cores occur in pairs with each pyrrole ring. Figure 7 also shows the pattern of close atoms between the two rings: the C_a atoms are close to either another C_a atom or to a C_m atom. The interatomic separations of the six unique carbon atoms of the inner 16-membered ring are only 3.31–3.39 Å, and the average value is 3.34 Å. The observed twist angle between the two rings, 31.3°, is necessary to allow both C_a···C_a and C_a···C_m close contacts. Larger values of this twist angle will lead to closer C_a···C_a contacts and longer C_a···C_m contacts, while smaller values of this twist angle lead to larger interatomic separations for all C_a and C_m atoms. A similar inter-ring separation is observed[30] in the $[Ru(OEP)]_2$ dimer that is held together by the short Ru=Ru double bond. The twist angle between the two rings is 22.7°, and the inter-ring C_a and C_m contacts are larger. No bond length alternation in the core is observed.

This apparent localization of bonding in the porphyrin core of $[Zn(OEP^{\bullet})(OH_2)]ClO_4$ is presumably due to the effects of dimerization, whose tightness and spin coupling suggests a new kind of interaction, best described as a new type of nonclassical bond. Indeed, the known, large enthalpy of dimerization (−17 kcal/mol),[23c] significant spectral changes upon dimerization,[23] and complete loss of paramagnetism from the radical are all consistent with the notion of forming a new compound. Interestingly, it can be noted that similar spectral changes have been seen upon dimerization (in solution) of the $[Mg(OEP^{\bullet})]^+$ radical cation and a similar solid-state structure would be predicted. To our knowledge, only the magnesium and zinc octaethylporphyrin radical compounds show the strongly red-shifted visible band attributed to dimer formation. The precise nature of the inter-ring bond(s) in $[Zn(OEP^{\bullet})(OH_2)]_2(ClO_4)_2$ will probably require a detailed ab initio calculation for a definitive description. The simplest expectation, that of predominant C_a–C_a interactions (since the C_a carbon atoms have the largest spin density of an a_{1u} radical and alternate in sign[27]), is clearly not realized. However, with an individual porphyrin ring the expected increase (for an A_{1u} radical) in the C_a–C_b bond distances is seen: the average distance is 1.467 (2) Å, about 0.02 Å longer than those of neutral metalloporphyrin complexes.[29]

Although crystalline $[Zn(OEP^{\bullet})(OH_2)]_2(ClO_4)_2$ is cleanly diamagnetic over the temperature range 6–300 K, the solid does exhibit a weak isotropic EPR signal with $g = 2.009$. This signal apparently is a related example of a phenomenon reported by Kivelson: diamagnetic phthalocyanines give (appreciable) solid-state EPR signals that are not attributable to the presence of impurities.[31] The cause of such signals remains, to our knowledge, unexplained. The infrared spectrum of $[Zn(OEP^{\bullet})(OH_2)]_2(ClO_4)_2$ show a weak doublet in the region that has been assigned[32] as diagnostic for radical formation. However, the infrared spectrum is quite similar to that reported by Itoh et al.[33] for $[Zn(OEP^{\bullet})]Br$. It is possible that the observed weak doublet for the radical marker band is also diagnostic for the alternant bonds in the core.

$[Ni(OEP)]ClO_4$. The most interesting feature of the $[Ni(OEP)]ClO_4$ system is the appearance of a cofacial $[Ni(OEP)]_2(ClO_4)_2$ dimer isolated as a crystalline solid. Like the zinc system, the two rings of the dimer are not laterally slipped with respect to each other. However, the nickel dimer does have several quite distinctively different structural features compared to the zinc dimer. Most importantly, these include a domed core conformation as can be seen in Figures 6 and 4 rather than the planar cores observed for $[Zn(OEP^{\bullet})(OH_2)]_2(ClO_4)_2$. The interplanar spacings are also different in the two complexes. In $[Zn(OEP^{\bullet})(OH_2)]_2(ClO_4)_2$, the interplanar spacing is the quite close 3.31 Å previously noted. In $[Ni(OEP)]_2(ClO_4)_2$, however, the *average* interplanar spacing is substantially shorter at 3.19 Å. Moreover, the separation between the two N_4 planes is only 3.08 Å, and there are inter-ring C_a···C_a distances as short as 3.14 Å. Of course, the C_b atoms saucer away from each other, but even at the ring extremity the perpendicular separation is still just 3.30 Å. The two rings (2-fold related) are essentially parallel with a dihedral angle of 0.2°. That there must be real bonding interactions between the two porphyrin rings can be clearly seen by noting that the short C_a···C_a distances of ~3.14 Å are almost as short as the 3.09-Å C···C distances found[34] between the benzene

(27) Gouterman, M. *J. Mol. Spectrosc.* **1961**, *6*, 138.
(28) Spaulding, L. D.; Eller, P. G.; Bertrand, J. A.; Felton, R. H. *J. Am. Chem. Soc.* **1974**, *96*, 982.
(29) Scheidt, W. R. In *The Porphyrins*; Dolphin, D., Ed.; Academic Press: New York, 1978; Vol. III, pp 463–511. Hoard, J. L. In *Porphyrins and Metalloporphyrins*; Smith, K. M., Ed.; Elsevier: Amsterdam, 1976.
(30) Collman, J. P.; Barnes, C E.; Sweptson, P. N.; Ibers, J. A. *J. Am. Chem. Soc.* **1984**, *106*, 3500.
(31) Neiman, R.; Kivelson, D. *J. Chem. Phys.* **1961**, *35*, 162.
(32) Shimomura, E. T.; Phillippi, M. A.; Goff, H. M.; Scholz, W. F.; Reed, C. A. *J. Am. Chem. Soc.* **1981**, *103*, 6778.
(33) Itoh, K.; Nakahasi, K.; Taeda, H. *J. Phys. Chem.* **1988**, *92*, 1464.
(34) Brown, C. J. *J. Chem. Soc.* **1953**, 3256. Lonsdale, K.; Milledge, H. J.; Rao, K. V. *Proc. R. Soc. London, Ser. A* **1960**, *255*, 82.

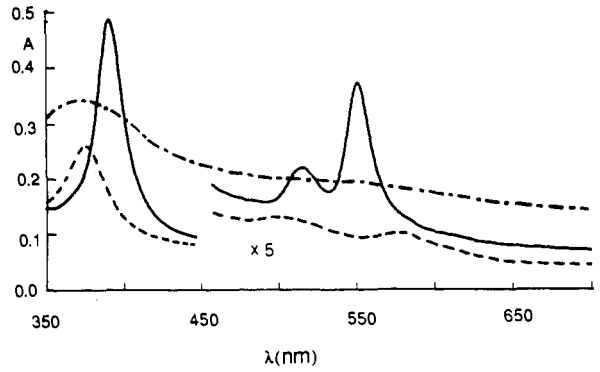

Figure 8. UV–vis spectra of Ni(OEP) in CH_2Cl_2 solution (solid line) and oxidized Ni(OEP) in CH_2Cl_2 solution (dashed line) and in the solid state (dot–dash). The two solution species are at the same concentration.

ring carbon atoms in [2.2]paracyclophane and for which a considerable strain energy is estimated.

We interpret these differences in core conformation as resulting from another significant difference between the two complexes. In the zinc dimer, the two zinc atoms are displaced 0.21 Å out-of-plane *away* from each other, while in the nickel complex the nickel atoms are displaced 0.09 Å out-of-plane *toward* each other. The Ni···Ni separation of 3.011 (4) Å and other structural features suggest the formation of a metal–metal interaction that is clearly absent in the zinc species.

Metal–metal-bonded porphyrin systems are relatively rare,[35] and only two such systems have been previously structurally characterized: the homonuclear dimer $[Ru(OEP)]_2$[30] and the heterobinuclear system [(OEP)Rh–In(OEP)].[36] The ruthenium complex has a metal–metal double bond, while the rhodium–indium complex is described as having a dative single bond. In Table VI, we collect a number of structural parameters that describe the interactions between the pair of rings in these two species and $[Ni(OEP)]_2(ClO_4)_2$ and $[Zn(OEP^{\bullet})(OH_2)]_2(ClO_4)_2$. The features of the nickel system, especially the doming of the core, are clearly consistent with the presence of a metal–metal interaction rather than simply the π–π interactions of the zinc system.

It should be noted that the 3.01-Å Ni···Ni separation is much longer than the Ni–Ni bonds found in ligand-bridged complexes, which are as short as 2.38 Å.[37] The Ni–Ni distance is similar to those of two previously characterized dimeric nickel macrocyclic species,[38,39] which have distances of 2.788 and 3.063 Å. These species are obtained by oxidative dehydrogenation of monomeric nickel(II) tetraaza[14]anulenes. Indeed, the bonding between the two metalloporphyrin halves of the $[Ni(OEP)]_2(ClO_4)_2$ dimer might be thought to be similar to that which has been proposed[38,39] for these two macrocyclic systems: nickel–nickel σ and δ bonds as well as weak π bonds between the two *eclipsed* macrocyclic ligands. However, such a bonding scheme is inappropriate for $[Ni(OEP)]_2(ClO_4)_2$, since the 40° twist of the two porphyrin rings means that the system has symmetry inappropriate for a bonding Ni–Ni δ interaction. Rather, the symmetry of the nickel porphyrin dimer is appropriate only for a Ni–Ni σ bond.

A σ bond of this type could result from the interaction of two d^7 nickel(III) atoms, each with a half-filled d_{z^2} orbital. Thus, the presence of a Ni–Ni bonding interaction suggests that this species could be formulated as containing Ni(III) ions. The formation of nickel(III) species could result from oxidation of the metal ion rather than the porphyrin ligand. It should be recalled that valence tautomerism (i.e., nickel(III) and a π-cation radical) has been discussed previously[40–43] for the oxidation product of nickel(II)

Table VI. Comparison of Four Binuclear M(OEP) Systems

complex	M–M[a]	Ct···Ct[a,b]	interplanar separation[a]	Ct···M[a]	Δ[a,c]	M–N$_p$[a]	interplanar angle[e]	twist angle[e,f]	approx core conform	av absolute displace[a,g]	max displace[a,g]	inter-ring separation[a,h] N–N	C_a–C_a	C_a–C_m	C_b–C_b	ref
$[Ru(OEP)]_2$	2.408 (1)	3.01	3.26	0.30	0.43	2.050	0.2	22.7	C_{4v}-domed	0.08, 0.10	0.21, 0.24	3.11	3.29	3.22	3.43	30
[(OEP)Rh–In(OEP)]	2.584 (1)	3.42	3.49	0.01	0.04	2.036	1.4	23.8	modest ruffling	0.07	0.19	3.43	3.54	3.52	3.48	36
				0.83	0.88	2.202										
$[Zn(OEP^{\bullet})(H_2O)]_2^{2+}$	3.789 (1)	3.29	3.31	−0.25[d]	−0.24[d]	2.051	0.0	31.3	planar	0.02	0.05	3.46	3.30	3.31	3.49	this work
$[Ni(OEP)]_2^{2+}$	3.011 (4)	3.08	3.19	0.04	0.09	1.949	0.2	40.4	C_{4v}-domed	0.05	0.14	3.36	3.14	3.22	3.66	this work

[a] Value in Å. [b] Ct is the center of the four nitrogen atoms of a porphyrin ring. [c] Metal atom displacement from mean plane of the 24-atom core. [d] Negative displacement indicates metal atom away from center of two rings. [e] Value in degrees. [f] Average of the N–M–M′–N′ dihedral angles. [g] Average absolute values from 24-atom mean plane. [h] Minimum value.

(35) Guilard, R.; Kadish, K. M. *Comments Inorg. Chem.* **1988**, *7*, 287.
(36) Jones, N. L.; Carroll, P. J.; Wayland, B. B. *Organometallics* **1986**, *5*, 33.
(37) Corbett, M.; Hoskins, B. *J. Chem. Soc., Chem. Commun.* **1969**, 1602.
(38) Peng, S.-M.; Goedken, V. L. *J. Am. Chem. Soc.* **1976**, *98*, 8500.
(39) Peng, S.-M.; Ibers, J. A.; Millar, M.; Holm, R. H. *J. Am. Chem. Soc.* **1976**, *98*, 8037.
(40) Wolberg, A.; Manassen, J. *Inorg. Chem.* **1970**, *9*, 2365.

tetraphenylporphyrin. It should also be noted that one direct attempt to characterize such valence tautomerism for oxidized nickel(II) octaethylporphyrin was unsuccessful.[41b] Moreover, our spectroscopic characterization of $[Ni(OEP)]_2(ClO)_4)_2$ is inconsistent with such a σ-bonded system. The UV–vis spectra of oxidized NiOEP (Figure 8) are those expected for a π-cation radical[3,44] and are comparable in dilute solution ($\sim 10^{-6}$ M) and the solid state. Hence, these spectra are also inconsistent with a simple description of interacting Ni(III) halves and neutral porphyrin rings.

The variation in the twist angle between the two rings of the four systems listed in Table VI may reflect differences in the bonding interactions between the two metalloporphyrin rings as well as the differences in interatomic repulsion. We had previously noted some of the inter-ring interactions of the $[Zn(OEP^{\bullet})(OH_2)]_2(ClO_4)_2$ system that suggest inter-ring bonding. The $[Ni(OEP)]_2^{2+}$ system also shows some inter-ring structural features that strongly suggest some type of π–π interaction. The twist angles of the first two metal–metal-bonded systems appear to have values appropriate for simultaneously allowing relatively close inter-ring plane–plane distances *and* maximizing nonbonded inter-ring atom–atom separations.[45] For these two complexes the inter-ring atom–atom separations increase from the ring center to the periphery. The remaining two complexes display curious reversals in the progression of these separations. Thus, the separations for $[Zn(OEP^{\bullet})(OH_2)]_2(ClO_4)_2$ decrease from the 3.46-Å N···N inter-ring separation to give C_a–C_a and C_a–C_m distances of ~3.3 Å. These distances appear to correlated with the unusual alternation in the bond distances of the ring previously described. The corresponding inter-ring distances in the nickel complex are even more unusual. All eight C_a–C_a distances are extremely short and range from 3.14 to 3.22 Å with an average value of 3.17 Å. Moreover, as is readily seen from Figure 5, the C_a atoms are almost directly overlapped with each other in the two rings. If the nickel complex is an a_{1u} radical, it is just these α-carbon atoms that have the major share of unpaired electron density[27] and would be expected to be the positions of strongest overlap for the formation of an extended π–π interaction between two rings. We thus conclude from the structural data that the interaction between the two oxidized $[Ni(OEP)]^+$ units must involve both bonding interactions between the two porphinato rings and the two metal ions.

Not unexpectedly for such tight π–π coupling, both compounds appear to be very strongly antiferromagnetically coupled. While the zinc complex is clearly diamagnetic, the nickel dimer does show a temperature-dependent magnetic moment of unknown origin. The magnitude of this paramagnetism varies with sample preparation and sample history, increasing with sample age. While every effort was made to obtain data on a freshly prepared sample, a few minutes aging was unavoidable. In addition, an EPR signal was observed for solid and solution $[Ni(OEP)]_2(ClO_4)_2$ (at g = 2.002) with an apparently larger intensity that that of the zinc complex. However, we believe that the paramagnetism is artifactual, resulting from production of a magnetic species during crystal decomposition. We note that the closely related species $[Ni(OEP)]SbCl_6$, although not analytically pure, was found to be diamagnetic.[46] In addition, both of the nickel tetraaza macrocycles[38,39] are diamagnetic.

The average Ni–N_p bond length is 1.949 (6) Å, a value commensurate with those of other nickel porphyrin complexes. This value is slightly shorter than the 1.96-Å value for planar Ni(OEP) complexes[47,48] and longer than the 1.930-Å value for a strongly S_4-ruffled derivative.[49] Thus, the molecular oxidation has not materially changed the geometry of the nickel–porphyrin interaction although it is to be noted that all[47-56] four-coordinate nickel(II) porphyrin complexes have the nickel(II) ion centered in the porphyrin plane.

Averaged values for the bond parameters of the core are shown in Figure 3b. The number in parentheses following each averaged value is the esd calculated on the assumption that all values are drawn from the same population. There is clearly some dispersion in the populations. However, the $[Ni(OEP)]ClO_4$ complex does not apparently show the localized alternating bonds of the inner 16-membered ring that was observed in $[Zn(OEP^{\bullet})(OH_2)]ClO_4$. In part, the metrical accuracy of the $[Ni(OEP)]ClO_4$ structure vitiates the significance of this lack. Consequently, we are unable to offer any conclusions concerning the effects of the relative twist orientations of the two rings with respect to this bond length alternation.

Summary. The one-electron oxidation products of Zn(OEP) and Ni(OEP) are both found to form strongly coupled dimeric structures that differ from each other in the detailed nature of the inter-ring bonding. The nickel system displays evidence for both Ni–Ni and inter-ring coupling, while the zinc system forms a tight dimer that is supported only by the inter-ring π–π interaction. The orbital interactions for these inter-ring couplings must be significantly different, since the relative orientations of the porphyrin rings lead to distinctively different inter-ring atom–atom contacts in the two complexes. Whether additional dimeric interaction patterns exist in other oxidized porphyrin dimers is a matter of active investigation.

Acknowledgments. W.R.S. and H.S. thank Prof. J. L. Sessler for a generous gift of H_2OEP. We acknowledge, with thanks, the support of the National Institutes of Health under Grants GM-38401 to W.R.S. and GM-23851 to C.A.R.

Supplementary Material Available: Tables SI–SVII, listing complete crystallographic details, anisotropic thermal parameters, fixed hydrogen atom positions, and magnetic susceptibility data for $[Zn(OEP^{\bullet})(OH_2)]_2(ClO_4)_2 \cdot 2C_2H_4Cl_2$ and $[Ni(OEP)]_2(ClO_4)_2 \cdot 8CH_2Cl_2$ (6 pages); tables of observed and calculated structure factor amplitudes (×10) for both complexes (28 pages). Ordering information is given on any current masthead page.

(41) (a) Dolphin, D. H.; Niem, T.; Felton, R. H.; Fujita, I. *J. Am. Chem. Soc.* **1975**, *97*, 5288. (b) Johnson, E. C.; Niem, T.; Dolphin, D. H. *Can. J. Chem.* **1978**, *56*, 1381.
(42) Kim, D.; Miller, L. A.; Spiro, T. G. *Inorg. Chem.* **1978**, *25*, 2468.
(43) Chang, D.; Malinski, T.; Ulman, A.; Kadish, K. M. *Inorg. Chem.* **1984**, *23*, 817.
(44) Unlike the zinc dimer, the nickel comlex shows only a very weak absorption at ~900 nm. We thank Dr. J. Fajer for this measurement.
(45) A twist angle of 0° leads to a completely eclipsed inter-ring structure, while a 45° twist angle will lead to all C_a atoms being overlapped. A value halfway between these limiting values is seen to best minimize inter-ring atomic separations for any value of the interplanar spacing.
(46) Erler, B. S. Ph.D. Thesis, University of Southern California, 1985.
(47) Cullen, D. L.; Meyer, E. F., Jr. *J. Am. Chem. Soc.* **1974**, *96*, 2095.
(48) Brennan, T. D.; Scheidt, W. R.; Shelnutt, J. A. *J. Am. Chem. Soc.* **1988**, *110*, 3919.
(49) Meyer, E. F., Jr. *Acta Crystallogr., Sect. B* **1974**, *B28*, 2162.
(50) Hamor, T. A.; Caughey, W. S.; Hoard, J. L. *J. Am. Chem. Soc.* **1965**, *87*, 2305.
(51) Pettersen, R. C. *J. Am. Chem. Soc.* **1971**, *93*, 5629.
(52) Gallucci, J. C.; Sweptson, P. N.; Ibers, J. A. *Acta Crystallogr., Sect. B* **1982**, *B38*, 2134.
(53) Kutzler, F. W.; Sweptson, P. N.; Berkovitch-Yellin, Z.; Ellis, D. E.; Ibers, J. A. *J. Am. Chem. Soc.* **1983**, *105*, 2996.
(54) Suh, P. M.; Sweptson, P. N.; Ibers, J. A. *J. Am. Chem. Soc.* **1984**, *106*, 5164.
(55) Stolzenberg, A. M.; Glazer, P. A.; Foxman, B. M. *Inorg. Chem.* **1986**, *25*, 983.
(56) Fillers, J. P.; Ravichandran, K. G.; Abdalmuhdi, I.; Tulinsky, A.; Chang, C. K. *J. Am. Chem. Soc.* **1986**, *108*, 417.